Contrasting elastic properties of heavily B- and N-doped graphene, with random distributions including aggregates

Karolina Z. Milowska
*Institute of Theoretical Physics, Faculty of Physics, University of Warsaw, ul. Hoża 69, PL-00-681 Warszawa, Poland**

Magdalena Woińska
Faculty of Chemistry, University of Warsaw, ul. Pasteura 1, PL-02-093 Warszawa, Poland

(Dated: April 10, 2013)

We focused on elastic properties of B- and N-doped graphene in wide range of concentrations up to 20%. The Young's, bulk and shear moduli and Poisson's ratio have been calculated by means of the density functional theory for a representative set of supercells with disordered impurity patterns including aggregates. In contrast to earlier work, it is demonstrated that doping with nitrogen even strengthens the graphene layers, whereas incorporation of boron induces large structural and morphological changes seen in simulated STM images. Young's and shear moduli increase or decrease with the doping strength for nitrogen or boron, respectively, while bulk modulus and Poisson's ratio exhibit opposite trends. Elastic properties of samples for both types of impurities are strongly related to the electronic structures, especially for heavy doping (>12%). Local arrangements of dopants and an agregation or separation of impurities play crucial role in the determination of stiffness in the investigated systems. Interestingly, these findings are opossed for B- and N-contained samples.

PACS numbers: 31.15.A-, 31.15.E-, 81.05.ue, 62.20.F-, 68.37.Ef

I. INTRODUCTION

Nowadays graphene, a two-dimensional monolayer formed out of sp^2 hybridizated carbon atoms ordered in a honeycomb-like lattice, attracts a lot of attention owing to its unique properties. Due to the hexagonal symmetry, its valence and conduction bands cross and have linear dispersion at the so called K point; these bands determine semimetallic character of graphene and its extremely high electron mobility.[1,2] This, in connection with excellent mechanical properties, renders graphene to be an ideal candidate for applications in flexible electronics[3,4] and nanocomposites.[5,6] However, the ability of generating controllable band gap in graphene is a prerequisite for effective applications in transistor based electronic devices.[7] Therefore, an effective functionalization that would open the zero energy band gap in pristine graphene without significant deterioration of the remaining advantageous properties is searched for, and practically, any thinkable way of reaching this target is currently investigated. Substitutional doping, which refers to substitution of carbon atoms in graphene lattice by atoms with different number of valence electrons such as boron or nitrogen, could be a recipe to achieve this goal.[2,8]

Compared to carbon, nitrogen has one additional electron and boron lacks one, which means that these elements should act as electron donors and acceptors, respectively. Despite the poor environmental stability of chemically doped graphene,[9] there are many experimental and theoretical studies that show a possibility to prepare p- and n-type semiconductors by substituting these elements into graphene.[8,10–14] It has been previously shown that, the Fermi level shifts with respect to the valence band top or the conduction band bottom resulting from B or N functionalization, correspondingly, and the band gap opens.[9–11,15,16]. Boron doped graphene (BG) has been successfully synthesized using arc-discharge of graphite electrodes in the presence of H_2, He and B_2H_6[16,17] and by the chemical vapor deposition (CVD) using polystyrene and HBO_3.[9] Whereas, single- and a few layer nitrogen doped graphene (NG) have been synthesized by the CVD with NH_3[15,18] or CH_4N_2O[9] as nitrogen source and using the arc-discharge method in the presence of H_2 and C_5H_5N[16] or H_2 and NH_3.[16,17]

The BG and NG materials open various potential applications like in graphene-based back-gate field-effect transistors,[9] nanosensors,[19,20] fuel cells,[21] lithium ion batteries[22,23] or even hydrogen storage.[24] Therefore understanding the influence of substitutional doping, with boron and nitrogen, on graphene properties is proved to be crucial.

In contrast to other authors, we find that the boron-doped graphene shows opposite elastic properties with respect to the nitrogen-doped graphene. These effects are especially well pronounced in heavily doped samples, not studied theoretically so far but extensively used in tailoring electronic devices[2]. The effects of dopants aggregation and disorder play a huge role in the determination of Young's, bulk and shear moduli as well as the Poisson's ratio. In this work, we analyze many local arrangements of impurities in the graphene layer, starting from small concentrations and ending with 20%. Therefore, we extended our previous theoretical studies,[11] on electronic properties of these systems, to mechanical and structural behaviour at the parameters close to the technological conditions.

II. THEORETICAL METHODS

Our studies of functionalized graphene layer are based on *ab initio* calculations within the framework of the spin polarized density functional theory (DFT).[25,26] Generalized gradient approximation of the exchange-correlation functional in Perdew-Burke-Ernzerhof (PBE) parameterization has been applied.[27] Calculations have been performed using the SIESTA package.[28,29] Valence electrons have been represented with double zeta basis sets of orbitals localized on atoms, with polarization functions also included. The influence of core electrons has been accounted within the pseudopotential formalism. Norm-conserving Troullier-Martins nonlocal pseudopotentials[30] used in our studies were cast into the Kleinman-Bylander separable form.[31] The energy cut-off for the density on the real space grid has been set to 800 Ry. The Brillouin zone has been sampled in the 5x5x1 Monkhorst and Pack scheme.[32] Calculations were performed within the supercell scheme with the graphene layers separated by a distance of 80 Å, large enough to eliminate any interaction. Structural optimization has been conducted using the conjugate gradient algorithm to achieve the residual forces, acting on the atoms, lower than 0.001 eV/$\AA$.

We performed calculations for 5x5 supercells containing 25 graphene primitive unit cells (i.e., consisting of 50 atoms). Such supercell has been chosen in order to examine a wide range of dopants concentrations and a variety of possible distributions of the substituent atoms. In the described graphene supercell, one to ten B or N atoms have been introduced, leading to the corresponding concentration of 2-20%. In the case of two substituted atoms in a supercell, all eleven symmetrically nonequivalent configurations of atoms have been examined. In the remaining cases, twelve different randomly chosen configurations have been taken into account. For each sample at given concentration, and with unique dopants distribution nonequivalent to other samples, the elastic properties have been calculated and averaged at the end. The statistical spreads of obtained values, due to disorder and aggregation, are also presented.

We simulated the scanning tunneling microscopy (STM) images in order to analyze the doped graphene structures. These images, depicted in Figure 1, are calculated within the Tersoff-Hamann scheme[33] in the constant current mode with the bias voltage (V_{bias}) of 0.5 V, and visualized using WSxM code.[34] Tip shape and its electronic structure were not taken into account. Density of the tunneling current, resulting from the applied small bias voltage between the tip and the sample, is calculated according to the formula:[35]

$$\rho_{STM}(\vec{r}, V_{bias}) = \int_{E_F - eV_{bias}}^{E_F} \sum_{i}^{N_{band}} \sum_{\vec{k} \in BZ} |\varphi_{i,\vec{k}}(\vec{r})|^2 \delta(E_{i,\vec{k}} - E) dE, \quad (1)$$

where $\varphi_{i,\vec{k}}$ is the wave function associated with the E_i eigenvalues from the energetic window set by the integrand range which contain N_{band} states.

We obtained the elastic properties for all considered concentrations and symmetrically nonequivalent configurations of substituent atoms. All values for each concentration have been averaged over the investigated geometric configurations and compared with the relevant results for B or N substitutions. We applied the tensile strain to the functionalized graphene along the one of the lattice vectors in the graphene lattice plane and calculated the response. The most interesting quantity, namely the Young's modulus, has been determined on the basis of the stress tensor σ_{ii} and the strain ε_{ii} components as follows:

$$Y = \frac{\sigma_{ii}}{\varepsilon_{ii}}. \quad (2)$$

The volume of doped systems was calculated using the equation

$$V_o = a \cdot b \cdot \sin(\theta) \cdot 2\, \frac{r_S n_s + r_C (n - n_s)}{n} \quad (3)$$

where a and b are lattice constants, θ is the angle between them, r_C and r_S are van der Waals radii of C atom (equal to 0.17 nm) and substituents (equal to 0.155 nm for N and 0.192 nm for B). The numbers n_S and n count dopant atoms and all the atoms in the supercell, respectively. The Poisson's ratio was obtained according to the formula

$$\nu = -\frac{\Delta a}{a}\, \frac{b}{\Delta b}, \quad (4)$$

where Δa and Δb denote a change of the relevant lattice constant in the strained graphene layer. Bulk modulus (K) and shear modulus (G) (which could be easily derived from Eq. 2 and Eq. 4) are given, respectively, by

$$K = \frac{Y}{3(1 - 2\nu)}, \quad (5)$$

$$G = \frac{Y}{2(1 + \nu)}, \quad (6)$$

to complete a set of the elastic constants calculated in this work.

III. RESULTS AND DISCUSSION

A. Atomic and charge-density changes induced by doping

In our previous investigations,[11,12] we focused on studies of the stability and electronic structure of B- and N-doped graphene. We found that these structures are stable, therefore it is interesting to proceed with deeper insight into physical and chemical properties. Important

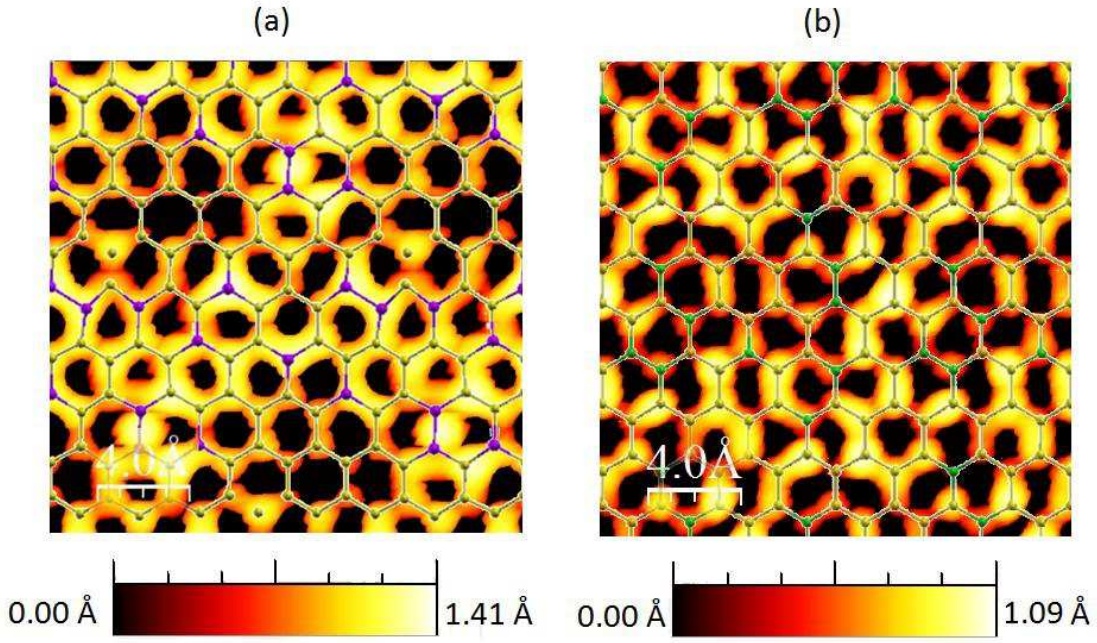

FIG. 1: (color online) Simulated STM images of graphene functionalized with B (a) and N (b) atoms are visualised above (V_{bias}=0.5V). Superimposed is a ball-and-stick model of the functionalized graphene lattice. The C atoms are depicted in yellow color, B in purple and N in green.

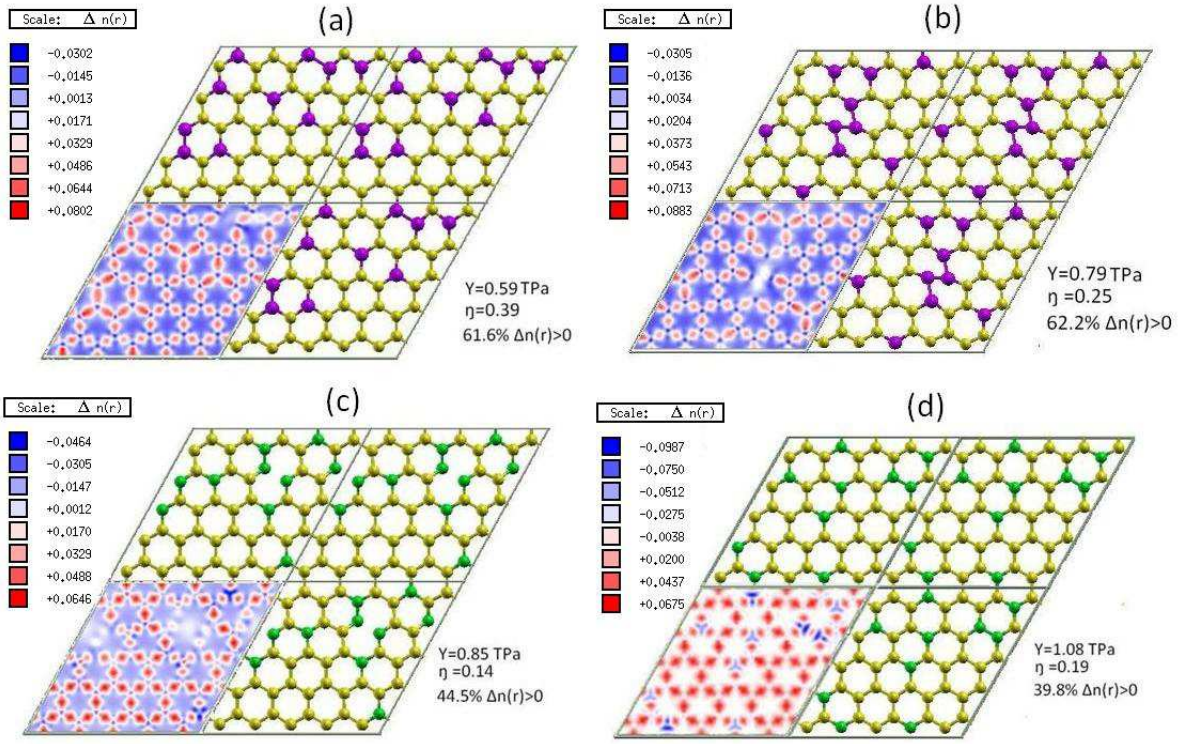

FIG. 2: (color online) The ball-and-stick model of four example structures of graphene functionalized boron (a,b) and nitrogen atoms (c,d) presented in three (5x5) supercells. In the bottom-left supercell the difference of the valence pseudocharge density and the superposition of spherical atomic valence pseudocharge densities (DRHO) is depicted. Concentration of substituent atoms: 20%.

TABLE I: Elastic properties of pure graphene and h-BN monolayers: Young's (Y), bulk (K) and shear modulus (G) [in TPa], and Poisson's ratio (ν), in comparison to the experimental and other theoretical values. Some papers give in-plane stiffness instead of Young's modulus, therefore, we have recalculated their results using as the layer thickness the Van der Waals radius of C atom for pure graphene or the averaged radius of N and B atoms for h-BN.

Property	graphene			h-BN		
	this work	calc.	exp.	this work	calc.	exp.
Y	1.050	0.965[39] 0.994[47]	0.980[42] 1[38]	0.756	0.769[39] 0.781,[47] 0.802[41] 0.829[40]	
K	0.528		0.582[43]	0.443		0.461[43]
G	0.449	0.432[47] 0.445[45] 0.366-0.460[46]	0.280[44]	0.311	0.323[47]	0.158[48]
ν	0.169	0.149[47] 0.16[39]		0.216	0.21[39] 0.211[47] 0.213[40] 0.217[41]	

conclusion from our earlier work was that substitution with boron atoms is energetically more favorable than substitution with nitrogen atoms, which is consistent with other theoretical work by Berseneva et al.[36]. We have also shown how functionalization induces morphological changes in these systems and leads to a redistribution of the electronic charge. Moreover, incorporation of foreign atoms not only destroys the sp^2 hybridization of the carbon atoms, but also causes deformations perpendicular to the graphene sheet. Boron atoms, in comparison to nitrogen impurities, have a greater influence on the geometry of doped graphene layer. Mostly, it is due to the fact that the covalent radius of boron is larger and that of nitrogen is similar to the radius of carbon. We have found that the graphene monolayer functionalized with boron atoms is no longer flat, and B atoms stick out from the surface. Similar observation has been also reported by other authors,[9,16,23] and this effect is better pronounced for higher concentrations of substituent atoms. The specified changes noticed in the morphology of functionalized graphene, their effect on the properties, and finally the wide range of potential applications, encouraged presented here studies of the elastic moduli.

Before we turn to the discussion of the elastic properties, we present shortly the structural and related electronic properties caused by the functionalization. Scanning tunneling microscopy (STM) is a very powerful experimental technique which allows to investigate simultaneously the electronic and atomic structure of samples. Therefore, we supplement our investigations with simulated STM images, which are presented in Figure 1 for graphene doped with boron (a) and nitrogen (b) at the bias voltage of 0.5 V. They provide useful information on the electron density of the occupied states. For high doping concentration of 20%, both images show deformed graphene structures, where impurities change the bond lengths and angles in lattice. We see dark holes corresponding to small current in the hexagon centers, which are very characteristic for the pure graphene[18,37] and originate from destructive interference between tip and C atoms. Boron-doped graphene presents large bright pattern centered on the B atoms, whereas nitrogen doped graphene is characterized by darker areas surrounding substituents. In the STM images, carbon atoms are brighter than nitrogen because the local charge density of N, at the distances pictured by this technique, has smaller contribution to ρ_{STM} than that originating from the first nearest neighbours of impurities. At the same time in B-doped graphene, the opposite situation resulting from the occupied antibonding states of both boron and its first C-neighbours can be observed. Similar pattern was obtained by Zheng[35]. It is worth mentioning, that our simulated STM images of the N-doped graphene correlate well with Zhao's STM mapping.[18]

From a picture for the differential charge-density (DRHO) shown in Figure 2 (insets), it is clear how the electronic structure changes under particular arrangements of impurities. If the dopants are more clustered, as in Figure 2(b) and (c), then the charge distribution is modified in larger areas than in the case of sparsely distributed substituents, as in Figure 2(a) and (d). Characteristic hexagons filled by negative differential charge-density and separated by positive differential density, which overlaps with bonds in most of the areas, cannot be clearly distinguished in the regions of clustered dopants. In the B-doped graphene, we observe the depletion of electron density in the B atoms vicinity and a transfer of the electronic charge to dopants and their first C-neighbors.

Due to one additional electron in N atoms as compared to carbon, in the N-doped graphene the electronic transfer from dopants to the C-rings is observed. In other words, N substituents induce strong intervalley electron scattering. Charge transfer between both types of substituents and the C atoms was also observed in some experiments[16,18] and theoretical works.[20,35] The differential charge-density of the doped system is much more locally affected by the presence of B atoms than by N atoms, which is consistent with the STM analysis.

B. Elastic properties of pure graphene and hexagonal boron nitride (h-BN) monolayer

As a starting point for further investigations of the elastic moduli of doped graphene, we present these quantities for pristine graphene and h-BN. The Young's, bulk, and shear moduli, and also Poisson's ratios for undoped

systems are gathered in Table I.

All theoretical results obtained by us and others are very close. There is also a good agreement with experimental data for Young's and bulk moduli. Discrepancy between theory and experiment is for shear moduli, where all theoretical values are about twice larger.

C. Elastic properties of graphene monolayer functionalized with boron and nitrogen atoms

We start with the presentation of Young's, bulk and shear moduli and Poisson's ratio for N- and B-doped graphene, in Figure 3.

Firstly, Young's modulus decreases with the increasing number of dopants, for both types of substituents, as shown in Figure 3(a). However, the reduction of this quantity in comparison to pure graphene is smaller for N-doped than for B-doped graphene. At the same time, the analysis of the geometric structure shows that boron induce more changes into the graphene layer than nitrogen atoms. For concentrations smaller than 14%, one can see that Young's modulus of NG is almost unchanged in comparison to the undoped structure. Our observations are in good agreement with Mortazavi's works, in which substituted nitrogen atoms do not remove flexibility of the graphene layer up to the concentration of 6%[49], whereas 4% of boron atoms reduce tensile strength by approximately 8% in comparison to pure graphene[50].

Starting from the concentration of 12%, the statistical spreads (depicted as error bars) for Young's modulus increase (Fig. 3 (a)), which means that the particular arrangement of dopants in graphene lattice starts to play an important role as far as stiffness of functionalized systems is concerned. To visualize this, see Figure 2 which displays four example structures of graphene doped with nitrogen and boron at the highest considered concentration of 20%. For this concentration, the differences between Young's moduli of symmetrically nonequivalent configurations are equal to 0.231 TPa for NG and 0.315 TPa for BG, respectively. Figure 2 (a) and (c) refer to the case of the smallest Young's modulus, whereas (b) and (d) to the case of the highest value of this elastic constant observed in the investigated systems. NG depicted in Figure 2(d) is characterized by Young's modulus higher than observed for the pure graphene. The stiffest structures of boron-doped graphene are those in which substituent atoms are aligned in the chains perpendicular to the direction of the applied tensile strain. In case of nitrogen-doped graphene, the structures characterized by the highest value of Young's modulus are those in which individual nitrogen atoms are surrounded by carbons, including the first and the second nearest neighbours. In our previous investigations of stability of boron and nitrogen doped graphene,[11] we have shown that the configuration in which dopants are more clustered is energetically less preferable than the configuration in which dopants are separated by carbon atoms. It was shown by Yuge[13] that creation of the B-B and N-N bonds is disfavored in comparison to forming of the B-C or N-C bonds.

There are also differences in the charge densities between particular arrangements of substituted atoms, clearly seen for higher concentrations. For a better comparison, near all structures in Figure 2, we have marked the participation of positive values [in %] of the difference between the valence pseudocharge density and a superposition of the atomic valence-pseudocharge densities at presented cross-sections of the substituted systems[53]. In the case of BG, the stiffer systems have higher concentration of positive charges in the cross-sections. Whereas in NG systems, Young's modulus is higher for these structures where higher electron density is observed.

Further, in Figure 3(b) and (c), we present results for bulk and shear moduli. The magnitude of which can be easily calculated using Young's modulus and Poisson's ratio, employing formulas 5 and 6, respectively. For concentration of dopants up to 16%, the bulk modulus does not display a significant dependency on boron or nitrogen doping and its average value is almost unchanged in comparison to the pure graphene. In contrast for higher concentrations, the average bulk modulus starts to increase for BG and decrease for NG with the increasing number of substituents. For the dopant concentration of 12% and higher, the difference between symmetrically nonequivalent configurations starts to be pronounced.

Shear modulus as a function of dopants, depicted in Fig. 3(c), is very similar to the Young's modulus (Figure 3(a)). Shear deformations, which play an important role in wrinkling and rippling behavior of graphene,[44,51] could be, like stiffness, related to the differences in local charge densities of doped systems. Particular arrangement of dopants in graphene layer, for concentration higher than 10%, affects the charge carrier scattering and the electron mobility. Shear modulus determines the resonance frequency of vibration modes involving torsional strains which, in contrast to the flexural strains, are not involved in thermoelastic loss.[52] It is important to note, that the NG-based devices are advantageous over the BG-based devices if one is interested in the mechanical quality factors.

The most striking result, which distinguishes properties of the n- and p-type doped graphene, shows up in Figure 3(d) which presents Poisson's ratio. This elastic property increases with the growing number of B atoms incorporated into the graphene layer and decreases with the increasing number of N atoms. Graphene layers doped with 20% of N atoms posses average Poisson's ratio almost the same as pure graphene (0.163). In contrast for 20% of B atoms, this quantity is even higher than for h-BN (0.315). This ratio, which describes how easily the system is deformed in the direction perpendicular to the applied load, allows to judge the difference between boron and nitrogen doped graphene in this respect. For the same applied stretching force, the B-doped graphene will contract in transverse direction much more than N-doped

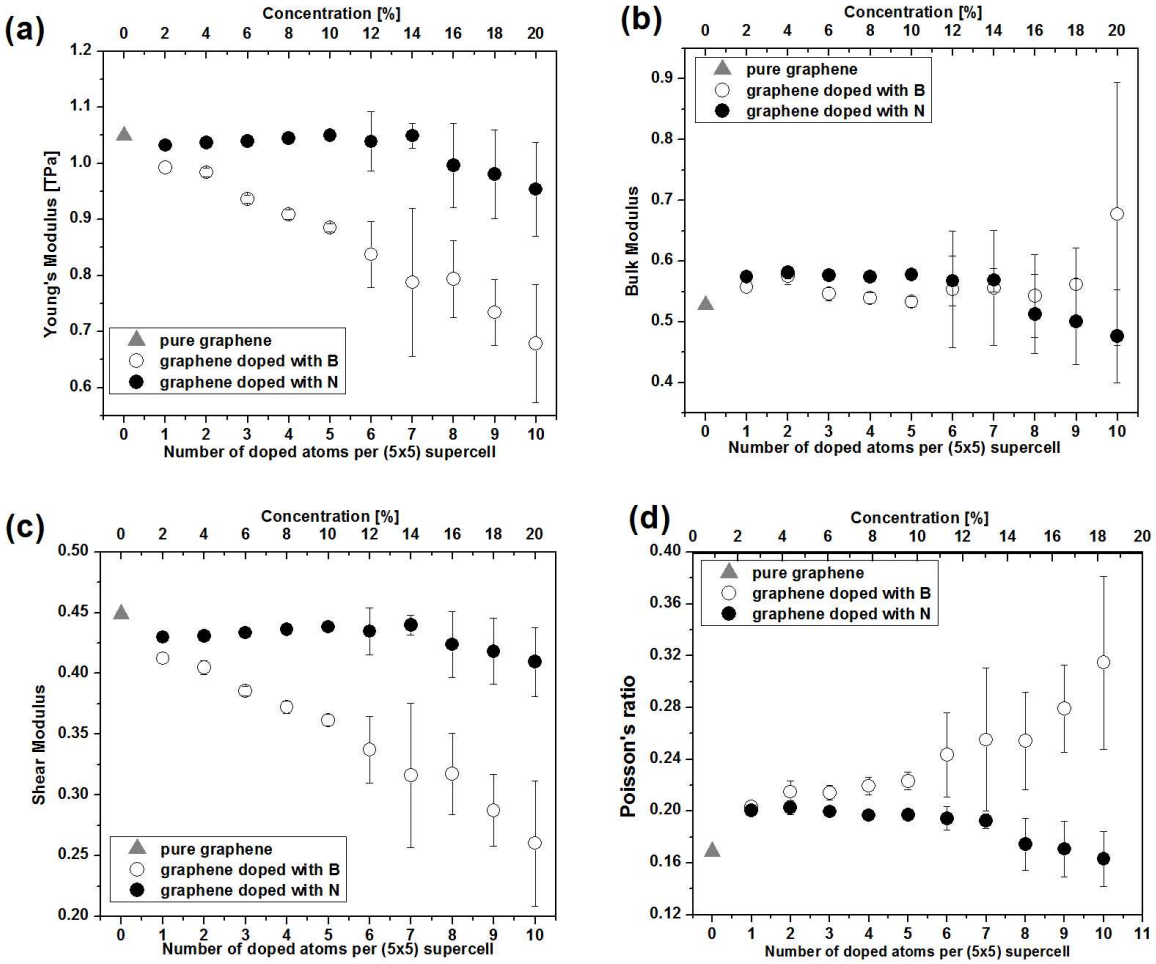

FIG. 3: Young's (a), bulk (b) and shear (c) moduli and Poisson's ratio (d) of (9,0) graphene functionalized with B (empty circles) and N (filled circles) as a function of the number of substituents per supercell and its percentage concentration (top x-axis). Symbols mean the averaged values obtained from different dopants arrangements in various supercells. The "error bars" are used to visualize the statistical spreads due to disorder.

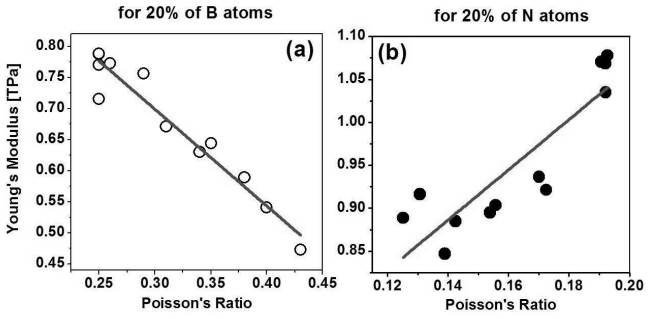

FIG. 4: The relation between Young's modulus and Poisson's ratio for all the symmetrically nonequivalent configurations at 20% concentration of boron (a) and nitrogen (b) atoms. Symbols mean values obtained from disordered samples.

graphene. For a better comparison of the differences between both systems, we present plots of Young's modulus vs Poisson's ratio for the highest considered concentration in Figure 4(a) and (b). Fitting a linear function to each case (using the least squares method), highlights two opposite tendencies: the slope is negative for the boron-doped graphene, whereas for the nitrogen-doped samples, this slope is positive.

IV. CONCLUSIONS

In this work, we present extensive and systematic studies of the elastic properties of B- and N-doped graphene. We investigated structures with 2-20% concentration of substituents in the graphene monolayer for various symmetrically nonequivalent configurations. Our ab-initio studies in the framework of density functional theory include, essential for creation of graphene-based devices, comparison between both type of dopants with respect to the concentration and particular arrangement of impu-

rities on graphene properties. The structure and related electronic properties of doped graphene have been investigated on the basis of the simulated STM images presenting samples morphology. Images of the differential densities between the valence pseudocharge and densities of the superposition of the atomic valence-pseudocharge (DRHO scheme) were also very helpful. We demonstrated that the B-doped graphene exhibits much larger morphological changes compared to the pure graphene than the N-doped samples.

Our studies also provide valuable theoretical predictions for elastic constants (Young's, shear and bulk moduli and Poisson's ratio) of doped graphene, and evidence clear chemical trends, shedding light on physical mechanisms governing these effects. From the analysis of disorder and aggregation, we observe a general rule that: aligning B atoms in the chains perpendicular to the applied tensile strain or surrounding individual N atoms by C-neighbours, including first and second nearest shell, builds samples with the highest Young's and shear moduli. We claim that some way of incorporating N atoms in the graphene layer could even strengthen the doped system in comparison to the pure graphene, whereas all B-type doping noticeably reduces the stiffness. Bulk modulus and the Poisson's ratio for the concentrations greater than 16% and 12%, respectively, exhibit opposite trends: the boron atoms improve the elastic constants while the nitrogen atoms worsen them. In the case of N-doped graphene, all of the considered elastic properties remain almost unchanged for concentrations smaller than 14%.

We have found that the elastic properties are strongly related to the electronic properties of doped systems, especially for heavily doped samples. Particular arrangement of dopants in graphene layer and the related local charge-densities play important role in mechanical quality factors in BG and NG. Each type of doping introduces different changes with respect to all considered properties, and these differences cannot be neglected.

The conclusions drawn in this work are important for the design of flexible electronics and nanocomposites or other applications in fields such as fuel cells or hydrogen storage, employing graphene layers.

V. ACKNOWLEDGMENTS

We would like to thank dr M. Wierzbowska for support and careful reading of the manuscript. The authors acknowledge financial support of the SiCMAT Project financed under the European Founds for Regional Development (Contract No. UDA-POIG.01.03.01-14-155/09). We thank also PL-Grid Infrastructure and Interdisciplinary Centre for Mathematical and Computational Modeling of University of Warsaw (Grant No. G47-5 and G47-16) for providing computer facilities.

* Electronic address: karolina.milowska@gmail.com

[1] A. K. Geim, K. S. Novoselov, Nature Mater. **6**, 183 (2007).
[2] V. Georgakilas , M. Otyepka, A. B. Bourlinos, V. Chandra, N. Kim, K. Ch. Kemp, P. Hobza, R. Zboril, K. S. Kim, Chem. Rev. **112**, 6156 (2012).
[3] J. S. Bunch, A. M. van der Zande, S. S. Verbridge, I. W. Frank, D. M. Tanenbaum, J. M. Parpia, H. G. Craighead, P. L. McEuen, Science **315**, 490 (2007).
[4] B. Standley, W. Bao, H. Zhang, J. Bruck, Ch. N. Lau, M. Bockrath, Nano Lett. **8**, 3345-3349 (2008).
[5] S. Stankovich, D. A. Dikin, G. H. B. Dommett, K. M. Kohlhaas, E. J. Zimney, E. A. Stach, R. D. Piner, S. T. Nguyen, R. S. Ruoff, Nature **442**, 282-286 (2006).
[6] T. Ramanathan, A. A. Abdala, S. Stankovich, D. A. Dikin, M. Herrera-Alonso, R. D. Piner, D. H. Adamson, H. C. Schniepp, X. Chen, R. S. Ruoff, S. T. Nguyen, I. A. Aksay, R. K. Prud'Homme, L. C. Brinson, Nature Nanotech. **3**, 327-331 (2008).
[7] F. Schwierz, Nature Nanotech. **3**, 487-496 (2010).
[8] H. Liu, Y. Liu, D. Zhuo, J. Mater. Chem. **21**, 3335-3345 (2011).
[9] T. Wu, H. Shen,L. Sun,B. Cheng, B. Liua and J. Shen, New J. Chem.,**36** , 1385-1391 (2012).
[10] S. Mukherjee, T. P. Kaloni, J. Nanopart. Res. **14**, 1059 (2012).
[11] M. Woinska, K. Z. Milowska, J. A. Majewski, http://arxiv.org/abs/1301.3956 (accepted in Phys. Stat. Sol.)
[12] M. Woinska, K. Z. Milowska, J. A. Majewski, Acta Physica Polonica A **122**, 1087-1089 (2012).
[13] K. Yuge, Phys. Rev. B, **79** 144109 (2009)
[14] A. Hanafusa, Y. Muramatsu, Y. Kaburagi, A. Yoshida, Y. Hishiyama, W. Yang, J. D. Denlinger, E. M. Gullikson, J. App. Phys. **110**, 053504 (2011).
[15] D. Wei, Y. Liu, Y. Wang, H. Zhang, L. Huang, G. Yu, Nano Lett. **9**, 1752-1758 (2009).
[16] L. S. Panchakarla, K. S. Subrahmanyam, S. K. Saha, A. Govindaraj, H. R. Krishnamurthy, U. V. Waghmare, C. N. R. Rao, Adv. Mater. **21**, 4726-4730 (2009).
[17] L. S. Panchakarla, A. Govindaraj, C. N. R. Rao, Inorganica Chimica Acta **363**, 4163-4174 (2010).
[18] L. Zhao, R. He, K. T. Rim, T. Schiros,K. S. Kim, H. Zhou,Ch. Gutirrez,S. P. Chockalingam, C. J. Arguello, L. Palova, D. Nordlund, M. S. Hybertsen, D. R. Reichman, T. F. Heinz,P. Kim, A. Pinczuk, G. W. Flynn, A. N. Pasupath, Science **333**, 999-1003 (2011).
[19] T. B. Martins, R. H. Miwa, A. J. R. da Silva, A. Fazzio, Phys. Rev. Lett. **98**, 196803 (2007).
[20] Y. Wang, Y Shao, D. W. Matson, J. Li, Y. Lin, ACS Nano **4** 1790-1798 (2010).
[21] L. Qu, Y. Liu, J.-B. Baek, L. Dai, ACS Nano **4**, 13211326 (2010).
[22] X. Wang, Z. Zeng, H. Ahn, G. Wang, Appl. Phys. Lett. **95**, 183103 (2009).
[23] S. Gao, Z. Ren., L. Wan, J. Zheng, P. Guo, Y. Zhou, App. Surf. Science **257**,7443 (2011).

[24] E. Beheshti, A. Nojeh, P. Servati, Carbon **49**, 1561-1567 (2011).
[25] P. Hohenberg, W. Kohn, Phys. Rev. **136**, 864 (1964).
[26] W. Kohn, L. J. Sham, Phys. Rev. **140**, A1133 (1965).
[27] J. P. Perdew, K. Burke, M. Ernzerhof, Phys. Rev. Lett. **77**, 3865 (1996).
[28] D. Sanchez-Portal, P. Ordejon, E. Artacho, J. M. Soler, Int. J. Quantum Chem. **65**, 453 (1997).
[29] J. M. Soler, E. Artacho, J. Gale, A. Garcia, J. Junquera, P. Ordejon, D. Sanchez-Portal, J. Phys.:Condens. Matter **14**, 2745 (2002).
[30] N. Troullier and J. L. Martins, Phys. Rev. B **43**, 1993 (1991).
[31] L. Kleinman and D. M. Bylander, Phys. Rev. Lett. **48**, 1425 (1982).
[32] H. D. Monkhorst and J. D. Pack, Phys. Rev. B **13**, 5188 (1976).
[33] J. Tersoff and D.R. Hamman Phys. Rev. Lett. **50**, 1998 (1983).
[34] I. Horcas, R. Fernandez, J.-M. Gomez-Rodrigez, J. Colchero, J. Gomez-Herrero, A. M. Baro Rev. Sci. Instrum. **78**, 013705 (2011)
[35] B. Zheng, P. Hermet and L. Henrard,ACS Nano, **4**, 4165 (2010).
[36] N. Berseneva, A. V. Krasheninnikov, R. M. Nieminen, Phys. Rev. Lett. **107**, 035501 (2011).
[37] H. Amara, S. Latil, V. Meunier, Ph. Lambin, J. -C. Charlier, Phys. Rev. B **76**, 115423 (2007).
[38] S. P. Koenig, N. G. Boddeti, M. L. Dunn, J. S. Bunch, Nature Nanotech. **6**, 543-546 (2011).
[39] M. Topsakal, S. Cahangirov, S. Ciraci, Applied Phys. Lett. **96**, 091912 (2010).
[40] M. Mirzenhard, R. Ansari, H. Rouhi, Superlatticies and Microstructures **53**, 223 (2013).
[41] Q. Peng, W. Ji, S. De, Comp. Mater, Sc. **56**, 11-17 (2012).
[42] C. Lee, X. Wei, J. W. Kysar, J. Hone, Science **321**, 385-388 (2008).
[43] A. Nag, K. Raidongia, K. P. S. S. Hembram, R. Datta, U. V. Waghmare, C. N. R. Rao, ACS Nano **4**, 1539-1544 (2010).
[44] X. Liu, T. H. Metcalf, J. T. Robinson, B. H. Houston, F. Scarpa, Nano Lett. **12**, 1013-1017 (2012).
[45] K. V. Zakharchenko, M. I. Katsnelson, A. Fasolino, Phys. Rev. Lett. **102**, 046808 (2009).
[46] K. Min, N. R. Aluru, Appl. Phys. Lett. **98**, 013113 (2011).
[47] K. N. Kudin, G. E. Scuseria, B. I. Yakobson, Phys. Rev. B **64**, 235406 (2001).
[48] T. Wittkowski, P. Cortina, J. Jorzick, K. Jung, B. Hillebrands, Diam. and Rel. Mater. **9**, 1957-1964 (2000).
[49] B. Mortazavi, S. Ahzi, V. Toniazzo, Y. Remond, Phys. Lett. A **376**, 1146 (2012)
[50] B. Mortazavi, S. Ahzi, Solid State Comm. (2012), http://dx.doi.org/10.1016/j.ssc.2012.04.048
[51] M. I. Katsnelson and A. K. Geim, A. Philos. Trans. R. Soc. A **366**, 195-204 (2008).
[52] B. H. Houston, D. M. Photiadis, M. H. Marcus, J. A. Bucaro, X. Liu, J. F. Vignola, App. Phys. Lett.**80(7)**, 1300-1303 (2002).
[53] The cross-sections have been chosen in such a way that they are in planes parallel to the graphene lattice with the perpendicular coordinate chosen so that it is an average position of all distorted atoms in the supercell.